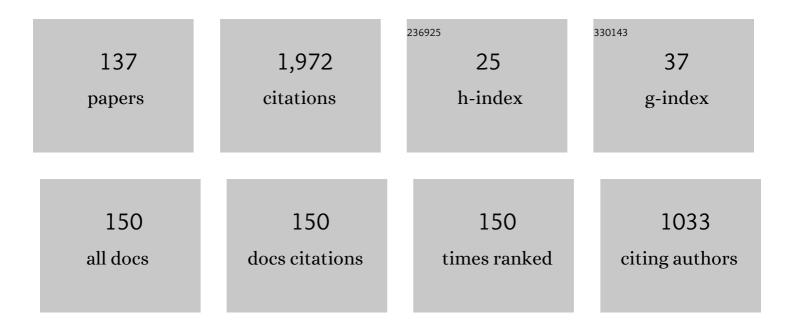
List of Publications by Year in descending order

Source: https://exaly.com/author-pdf/790275/publications.pdf Version: 2024-02-01



#	Article	IF	CITATIONS
1	Mode separation of Lamb waves based on dispersion compensation method. Journal of the Acoustical Society of America, 2012, 131, 2714-2722.	1.1	127
2	Measurement of the Dispersion and Attenuation of Cylindrical Ultrasonic Guided Waves in Long Bone. Ultrasound in Medicine and Biology, 2009, 35, 641-652.	1.5	93
3	Multiridge-based analysis for separating individual modes from multimodal guided wave signals in long bones. IEEE Transactions on Ultrasonics, Ferroelectrics, and Frequency Control, 2010, 57, 2480-2490.	3.0	75
4	Identification and analysis of multimode guided waves in tibia cortical bone. Ultrasonics, 2006, 44, e279-e284.	3.9	70
5	Sparse SVD Method for High-Resolution Extraction of the Dispersion Curves of Ultrasonic Guided Waves. IEEE Transactions on Ultrasonics, Ferroelectrics, and Frequency Control, 2016, 63, 1514-1524.	3.0	61
6	Analysis of frequency dependence of ultrasonic backscatter coefficient in cancellous bone. Journal of the Acoustical Society of America, 2008, 124, 4083-4090.	1.1	47
7	Analysis of Apparent Integrated Backscatter Coefficient and Backscattered Spectral Centroid Shift in Calcaneus inAvivo for the Ultrasonic Evaluation of Osteoporosis. Ultrasound in Medicine and Biology, 2014, 40, 1307-1317.	1.5	42
8	Measurements of ultrasonic phase velocities and attenuation of slow waves in cellular aluminum foams as cancellous bone-mimicking phantoms. Journal of the Acoustical Society of America, 2011, 129, 3317-3326.	1.1	41
9	Analysis of Superimposed Ultrasonic Guided Waves in Long Bones by the Joint Approximate Diagonalization of Eigen-matrices Algorithm. Ultrasound in Medicine and Biology, 2011, 37, 1704-1713.	1.5	41
10	Transmission analysis of ultrasonic Lamb mode conversion in a plate with partial-thickness notch. Ultrasonics, 2014, 54, 395-401.	3.9	41
11	Joint Optimization of Trajectory, Propulsion, and Thrust Powers for Covert UAV-on-UAV Video Tracking and Surveillance. IEEE Transactions on Information Forensics and Security, 2021, 16, 1959-1972.	6.9	39
12	The relationship between ultrasonic backscatter and trabecular anisotropic microstructure in cancellous bone. Journal of Applied Physics, 2014, 115, .	2.5	36
13	Wideband dispersion reversal of lamb waves. IEEE Transactions on Ultrasonics, Ferroelectrics, and Frequency Control, 2014, 61, 997-1005.	3.0	36
14	Automatic mode extraction of ultrasonic guided waves using synchrosqueezed wavelet transform. Ultrasonics, 2019, 99, 105948.	3.9	35
15	Experimental demonstration of underwater ultrasound cloaking based on metagrating. Applied Physics Letters, 2020, 117, .	3.3	35
16	Ultrasonic sharp autofocusing with acoustic metasurface. Physical Review B, 2020, 102, .	3.2	34
17	High-resolution Lamb waves dispersion curves estimation and elastic property inversion. Ultrasonics, 2021, 115, 106427.	3.9	34
18	Low-intensity pulsed ultrasound prevents muscle atrophy induced by type 1 diabetes in rats. Skeletal Muscle, 2017, 7, 29.	4.2	32

#	Article	IF	CITATIONS
19	Spectral ratio method to estimate broadband ultrasound attenuation of cortical bones <i>in vitro</i> using multiple reflections. Physics in Medicine and Biology, 2007, 52, 5855-5869.	3.0	31
20	Assessment of the Fundamental Flexural Guided Wave in Cortical Bone by an Ultrasonic Axial-Transmission Array Transducer. Ultrasound in Medicine and Biology, 2013, 39, 1223-1232.	1.5	31
21	Signal of Interest Selection Standard for Ultrasonic Backscatter in Cancellous Bone Evaluation. Ultrasound in Medicine and Biology, 2015, 41, 2714-2721.	1.5	31
22	Measurement of tortuosity in aluminum foams using airborne ultrasound. Ultrasonics, 2010, 50, 1-5.	3.9	29
23	Multichannel processing for dispersion curves extraction of ultrasonic axial-transmission signals: Comparisons and case studies. Journal of the Acoustical Society of America, 2016, 140, 1758-1770.	1.1	29
24	Full-Matrix Phase Shift Migration Method for Transcranial Ultrasonic Imaging. IEEE Transactions on Ultrasonics, Ferroelectrics, and Frequency Control, 2021, 68, 72-83.	3.0	29
25	Deep Learning Analysis of Ultrasonic Guided Waves for Cortical Bone Characterization. IEEE Transactions on Ultrasonics, Ferroelectrics, and Frequency Control, 2021, 68, 935-951.	3.0	28
26	Relationships of Ultrasonic Backscatter With Bone Densities and Microstructure in Bovine Cancellous Bone. IEEE Transactions on Ultrasonics, Ferroelectrics, and Frequency Control, 2018, 65, 2311-2321.	3.0	27
27	Simplified inverse filter tracking algorithm for estimating the mean trabecular bone spacing. IEEE Transactions on Ultrasonics, Ferroelectrics, and Frequency Control, 2008, 55, 1453-1464.	3.0	26
28	Effect of selected signals of interest on ultrasonic backscattering measurement in cancellous bones. Science China: Physics, Mechanics and Astronomy, 2013, 56, 1310-1316.	5.1	25
29	Coded excitation of ultrasonic guided waves in long bone fracture assessment. Ultrasonics, 2014, 54, 1203-1209.	3.9	25
30	Ray Theory-Based Transcranial Phase Correction for Intracranial Imaging: A Phantom Study. IEEE Access, 2019, 7, 163013-163021.	4.2	23
31	The analysis and compensation of cortical thickness effect on ultrasonic backscatter signals in cancellous bone. Journal of Applied Physics, 2014, 116, .	2.5	20
32	Quantification of guided mode propagation in fractured long bones. Ultrasonics, 2014, 54, 1210-1218.	3.9	20
33	Nonlinear Inversion of Ultrasonic Dispersion Curves for Cortical Bone Thickness and Elastic Velocities. Annals of Biomedical Engineering, 2019, 47, 2178-2187.	2.5	19
34	Therapeutic Effects of Low-Intensity Pulsed Ultrasound on Osteoporosis in Ovariectomized Rats: Intensity-Dependent Study. Ultrasound in Medicine and Biology, 2020, 46, 108-121.	1.5	19
35	Feasibility of Bone Assessment with Ultrasonic Backscatter Signals in Neonates. Ultrasound in Medicine and Biology, 2013, 39, 1751-1759.	1.5	18
36	Axial Transmission Method for Long Bone Fracture Evaluation by Ultrasonic Guided Waves: Simulation, Phantom and inÂVitro Experiments. Ultrasound in Medicine and Biology, 2014, 40, 817-827.	1.5	18

#	Article	IF	CITATIONS
37	Inhibition of MSTN signal pathway may participate in LIPUS preventing bone loss in ovariectomized rats. Journal of Bone and Mineral Metabolism, 2020, 38, 14-26.	2.7	18
38	A base-sequence-modulated golay code improves the excitation and measurement of ultrasonic guided waves in long bones. IEEE Transactions on Ultrasonics, Ferroelectrics, and Frequency Control, 2012, 59, 2580-3.	3.0	17
39	Ultrasonic backscatter measurements at the calcaneus: An in vivo study. Measurement: Journal of the International Measurement Confederation, 2018, 122, 128-134.	5.0	16
40	Modulation of Orbital-Angular-Momentum Symmetry of Nondiffractive Acoustic Vortex Beams and Realization Using a Metasurface. Physical Review Applied, 2020, 14, .	3.8	16
41	An Ultrasonic Backscatter Instrument for Cancellous Bone Evaluation in Neonates. Engineering, 2015, 1, 336-343.	6.7	15
42	Correlation between the combination of apparent integrated backscatter–spectral centroid shift and bone mineral density. Journal of Medical Ultrasonics (2001), 2016, 43, 167-173.	1.3	15
43	Wavelet transform-based photoacoustic time-frequency spectral analysis for bone assessment. Photoacoustics, 2021, 22, 100259.	7.8	15
44	Automated lung ultrasound scoring for evaluation of coronavirus disease 2019 pneumonia using two-stage cascaded deep learning model. Biomedical Signal Processing and Control, 2022, 75, 103561.	5.7	15
45	Measurement of the Human Calcaneus In Vivo Using Ultrasonic Backscatter Spectral Centroid Shift. Journal of Ultrasound in Medicine, 2016, 35, 2197-2208.	1.7	14
46	Longitudinal effects of low-intensity pulsed ultrasound on osteoporosis and osteoporotic bone defect in ovariectomized rats. Ultrasonics, 2021, 113, 106360.	3.9	14
47	Detection of collagen by multi-wavelength photoacoustic analysis as a biomarker for bone health assessment. Photoacoustics, 2021, 24, 100296.	7.8	14
48	Joint spectrogram segmentation and ridge-extraction method for separating multimodal guided waves in long bones. Science China: Physics, Mechanics and Astronomy, 2013, 56, 1317-1323.	5.1	13
49	Ultrasonic Backscatter Difference Measurement of Bone Health in Preterm and Term Newborns. Ultrasound in Medicine and Biology, 2020, 46, 305-314.	1.5	13
50	High-resolution bone microstructure imaging based on ultrasonic frequency-domain full-waveform inversion*. Chinese Physics B, 2021, 30, 014302.	1.4	13
51	Acoustic orbital angular momentum prism for efficient vortex perception. Applied Physics Letters, 2021, 118, .	3.3	13
52	Fourier-Domain Ultrasonic Imaging of Cortical Bone Based on Velocity Distribution Inversion. IEEE Transactions on Ultrasonics, Ferroelectrics, and Frequency Control, 2021, 68, 2619-2634.	3.0	13
53	Randomized Spatial Downsampling-Based Cauchy-RPCA Clutter Filtering for High-Resolution Ultrafast Ultrasound Microvasculature Imaging and Functional Imaging. IEEE Transactions on Ultrasonics, Ferroelectrics, and Frequency Control, 2022, 69, 2425-2436.	3.0	13
54	Experimental Observation of Cumulative Second-Harmonic Generation of Lamb Waves Propagating in Long Bones. Ultrasound in Medicine and Biology, 2014, 40, 1660-1670.	1.5	12

#	Article	IF	CITATIONS
55	Inhibition of myostatin signal pathway may be involved in low-intensity pulsed ultrasound promoting bone healing. Journal of Medical Ultrasonics (2001), 2019, 46, 377-388.	1.3	12
56	Characterization of multi-biomarkers for bone health assessment based on photoacoustic physicochemical analysis method. Photoacoustics, 2022, 25, 100320.	7.8	12
57	Fatigue evaluation of long cortical bone using ultrasonic guided waves. Journal of Biomechanics, 2018, 77, 83-90.	2.1	11
58	Numerical Evaluation of the Influence of Skull Heterogeneity on Transcranial Ultrasonic Focusing. Frontiers in Neuroscience, 2020, 14, 317.	2.8	11
59	MSTN is a key mediator for low-intensity pulsed ultrasound preventing bone loss in hindlimb-suspended rats. Bone, 2021, 143, 115610.	2.9	11
60	Broadband Three-Dimensional Focusing for an Ultrasound Scalpel at Megahertz Frequencies. Physical Review Applied, 2021, 16, .	3.8	11
61	Low-Intensity Pulsed Ultrasound Promotes Exercise-Induced Muscle Hypertrophy. Ultrasound in Medicine and Biology, 2017, 43, 1411-1420.	1.5	10
62	Simultaneous Segmentation of Fetal Hearts and Lungs for Medical Ultrasound Images via an Efficient Multi-scale Model Integrated With Attention Mechanism. Ultrasonic Imaging, 2021, 43, 308-319.	2.6	10
63	Artifact removal in photoacoustic tomography with an unsupervised method. Biomedical Optics Express, 2021, 12, 6284.	2.9	10
64	Ultrasound-Guided Detection and Segmentation of Photoacoustic Signals from Bone Tissue In Vivo. Applied Sciences (Switzerland), 2021, 11, 19.	2.5	10
65	A New Approach to Guided Wave Ray Tomography for Temperature-Robust Damage Detection Using Piezoelectric Sensors. Sensors, 2018, 18, 3518.	3.8	9
66	The Ability of Ultrasonic Backscatter Parametric Imaging to Characterize Bovine Trabecular Bone. Ultrasonic Imaging, 2019, 41, 271-289.	2.6	9
67	CM-SegNet: A deep learning-based automatic segmentation approach for medical images by combining convolution and multilayer perceptron. Computers in Biology and Medicine, 2022, 147, 105797.	7.0	9
68	Basic Study for Ultrasound-Based Navigation for Pedicle Screw Insertion Using Transmission and Backscattered Methods. PLoS ONE, 2015, 10, e0122392.	2.5	8
69	Three-dimensional ultrasound subwavelength arbitrary focusing with broadband sparse metalens. Science China: Physics, Mechanics and Astronomy, 2022, 65, 1.	5.1	8
70	Ultrasparse and omnidirectional acoustic ventilated meta-barrier. Applied Physics Letters, 2022, 120, .	3.3	8
71	Ultrasonic backscatter characterization of cancellous bone using a general Nakagami statistical model. Chinese Physics B, 2019, 28, 024302.	1.4	7
72	Ultrasonic Backscatter Technique for Assessing and Monitoring Neonatal Cancellous Bone Status in Vivo. IEEE Access, 2019, 7, 157417-157426.	4.2	7

#	Article	IF	CITATIONS
73	Bone Chemical Composition Assessment with Multi-Wavelength Photoacoustic Analysis. Applied Sciences (Switzerland), 2020, 10, 8214.	2.5	7
74	Spectrogram decomposition of ultrasonic guided waves for cortical thickness assessment using basis learning. Ultrasonics, 2022, 120, 106665.	3.9	7
75	Gross Tumor Volume Definition and Comparative Assessment for Esophageal Squamous Cell Carcinoma From 3D 18F-FDG PET/CT by Deep Learning-Based Method. Frontiers in Oncology, 2022, 12, 799207.	2.8	7
76	Study on synergistic effects of carboxymethyl cellulose and LIPUS for bone tissue engineering. Carbohydrate Polymers, 2022, 286, 119278.	10.2	7
77	Early severity prediction of BPD for premature infants from chest X-ray images using deep learning: A study at the 28th day of oxygen inhalation. Computer Methods and Programs in Biomedicine, 2022, 221, 106869.	4.7	7
78	Ellipse of uncertainty based algorithm for quantitative evaluation of defect localization using Lamb waves. Ultrasonics, 2022, 125, 106802.	3.9	7
79	Coded excitation speeds up the detection of the fundamental flexural guided wave in coated tubes. AIP Advances, 2016, 6, 095001.	1.3	6
80	A Combined Ultrasonic Backscatter Parameter for Bone Status Evaluation in Neonates. Computational and Mathematical Methods in Medicine, 2020, 2020, 1-9.	1.3	6
81	A Deep Learning Approach for the Photoacoustic Tomography Recovery From Undersampled Measurements. Frontiers in Neuroscience, 2021, 15, 598693.	2.8	6
82	Combined spectral estimator for phase velocities of multimode Lamb waves in multilayer plates. Ultrasonics, 2006, 44, e1145-e1150.	3.9	5
83	Multichannel wideband mode-selective excitation of ultrasonic guided waves in long cortical bone. , 2016, , .		5
84	Variability in Ultrasound Backscatter Induced by Trabecular Microstructure Deterioration in Cancellous Bone. BioMed Research International, 2018, 2018, 1-7.	1.9	5
85	Automated Identification and Localization of the Inferior Vena Cava Using Ultrasound: An Animal Study. Ultrasonic Imaging, 2018, 40, 232-244.	2.6	5
86	Imaging Spinal Curvatures of AIS Patients using 3D US Free-hand Fast Reconstruction Method. , 2019, , .		5
87	Bone Chemical Composition Analysis Using Photoacoustic Technique. Frontiers in Physics, 2020, 8, .	2.1	5
88	Long-distance shift of ultrasonic beam using a thin plate with periodic gratings. Ultrasonics, 2019, 95, 32-36.	3.9	4
89	Measuring Spinous Process Angle on Ultrasound Spine Images using the GVF Segmentation Method. , 2019, , .		4
90	Weight-bearing exercise prevents skeletal muscle atrophy in ovariectomized rats. Journal of Physiology and Biochemistry, 2021, 77, 273-281.	3.0	4

#	Article	IF	CITATIONS
91	Ultrasonic Backscatter Measurements of Human Cortical and Trabecular Bone Densities in a Head-Down Bed-Rest Study. Ultrasound in Medicine and Biology, 2021, 47, 2404-2415.	1.5	4
92	Nondestructive Evaluation of Special Defects Based on Ultrasound Metasurface. Frontiers in Materials, 2022, 8, .	2.4	4
93	Correlations between signal spectrum of ultrasonic backscatter and cancellous bone microstructure. , 2009, , .		3
94	Multichannel Crossed Convolutional Neural Network for Combined Estimation of Cortical Thickness and Bulk Velocities Using Ultrasonic Guided Waves: A Simulation Study. , 2019, , .		3
95	Improved Photoacoustic Imaging of Numerical Bone Model Based on Attention Block U-Net Deep Learning Network. Applied Sciences (Switzerland), 2020, 10, 8089.	2.5	3
96	Single Versus Multi-channel Dispersion Analysis of Ultrasonic Guided Waves Propagating in Long Bones. Ultrasonic Imaging, 2021, 43, 157-163.	2.6	3
97	Robust PCA-Based Clutter Filtering Method for Super-Resolution Ultrasound Localization Microscopy. , 2021, , .		3
98	Index-Rotated Fast Ultrasound Imaging of Cortical Bone Based on Predicted Velocity Model. IEEE Transactions on Ultrasonics, Ferroelectrics, and Frequency Control, 2022, 69, 1582-1595.	3.0	3
99	Photoacoustic characterization of bone physico-chemical information. Biomedical Optics Express, 2022, 13, 2668.	2.9	3
100	Simulation of propagation characteristics of ultrasonic guided waves in fractured long bone. , 2008, ,		2
101	Transverse and Oblique Long Bone Fracture Evaluation by Low Order Ultrasonic Guided Waves: A Simulation Study. BioMed Research International, 2017, 2017, 1-10.	1.9	2
102	A Free Plate Model Could Predict Ultrasonic Guided Waves Propagation in a 3D Printed Skull Phantom. , 2019, , .		2
103	Electric Field and Transmitting Power Analysis of Segmented and Unsegmented Loop Antennas for Transcutaneous Power Transfer. IEEE Transactions on Antennas and Propagation, 2021, 69, 3485-3492.	5.1	2
104	An Electromagnetic Fiber Acoustic Transducer with Dual Modes of Loudspeaker and Microphone. Small, 2021, 17, 2102052.	10.0	2
105	Extraction of the First-Arriving-Signal and Fundamental Flexural Guided Wave Using a Radon Transform Based Approach Applied to Ultrasonic Characterization of Cortical Bone. , 2021, , .		2
106	Cortical Bone Ultrasonic Imaging Based on Accurate Delay Times. , 2021, , .		2
107	A Robust Lamb Wave Imaging Approach to Plate-Like Structural Health Monitoring of Materials With Transducer Array Position Errors. IEEE Transactions on Ultrasonics, Ferroelectrics, and Frequency Control, 2022, 69, 2162-2177.	3.0	2
108	Characterization of Cancellous Bone Microstructure by Using Ultrasonic Apparent Backscatter Imaging. , 2009, , .		1

#	Article	IF	CITATIONS
109	Ultrasonic guided waves dispersion reversal for long bone thickness evaluation: A simulation study. , 2013, 2013, 1930-3.		1
110	Sparse inversion SVD method for dispersion extraction of ultrasonic guided waves in cortical bone. , 2015, , .		1
111	A Time-Frequency Independent Component Analysis Method for Group Velocity Extraction of Ultrasonic Guided Waves. , 2019, , .		1
112	Cortical Bone Fracture Imaging using Velocity Model Based Multistatic Synthetic Aperture Ultrasound. , 2019, , .		1
113	Analysis of Ultrasonic Guided Wave Propagation in Multilayered Bone Structure With Varying Soft-Tissue Thickness in View of Cortical Bone Characterization. IEEE Transactions on Ultrasonics, Ferroelectrics, and Frequency Control, 2022, 69, 147-155.	3.0	1
114	Frequency distillation with dispersive reflector for multitone ultrasound perception. Applied Physics Letters, 2021, 119, .	3.3	1
115	Randomized Spatial Downsampling based Robust PCA Clutter Filtering for Ultrafast Ultrasound Imaging. , 2021, , .		1
116	An Amplitude Modulation Ultrasonic Backscatter Method for Estimation Characterization of Cancellous Bones. , 2021, , .		1
117	Ex-vivo Ultrasonic Tomography Imaging of Cortical Bone Based on Velocity Model Prediction. , 2021, , .		1
118	Nonlinear inversion of ultrasonic guided waves for in vivo evaluation of cortical bone properties. Chinese Physics B, 2022, 31, 074301.	1.4	1
119	Bone Microstructure Evaluation by Photoacoustic Time-frequency Spectral Analysis. , 2020, , .		1
120	Real Time Waveguide Parameter Estimation Using Sparse Multimode Disperse Radon Transform. , 2021, , .		1
121	Improved Ultrasound Imaging Performance with Complex Cumulant Analysis. IEEE Transactions on Biomedical Engineering, 2022, PP, 1-1.	4.2	1
122	Meta-Learning Analysis of Ultrasonic Guided Waves for Coated Cortical Bone Characterization. IEEE Transactions on Ultrasonics, Ferroelectrics, and Frequency Control, 2022, 69, 2010-2027.	3.0	1
123	The Spectrum-Beamformer for Conventional B-Mode Ultrasound Imaging System: Principle, Validation, and Robustness. Ultrasonic Imaging, 2022, , 016173462210851.	2.6	1
124	Ultrasonic guided wave propagation in long bones with varying cortical thickness. , 2009, , .		0
125	Influence of signal selection on ultrasonic backscatter and in cancellous bone assessment. , 2015, , .		0
126	Effect of elastic modulus on the nonlinear ultrasonic Lamb waves in cortical bone: A numerical		0

study., 2015, , .

#	ARTICLE	IF	CITATIONS
127	Coded Excitation of Guided Ultrasonic Waves in Long Bone for Assessment of Fracture Depth. IFMBE Proceedings, 2018, , 53-58.	0.3	0
128	Application of Dynamic Time Warping Technique to Evaluate Microstructures of Cancellous Bones. , 2018, , .		0
129	Assessment of cortical bone fatigue using coded nonlinear ultrasound*. Chinese Physics B, 2021, 30, 094301.	1.4	0
130	Ability of Ultrasonic Apparent Backscatter to Reflect Cancellous Bone Densities. IFMBE Proceedings, 2018, , 69-73.	0.3	0
131	M-Sequence Excitation of Ultrasonic Backscatter Signals for Cancellous Bone Evaluation. IFMBE Proceedings, 2018, , 37-43.	0.3	0
132	Bone Health Assessment Using Photoacoustic Temporal Profile Analysis. , 2021, , .		0
133	Ultrafast Ultrasound Imaging for Micro-Nanomotors: A Phantom Study. , 2021, , .		0
134	Simulation of LIPUS Topography and the Thermal Properties of the Achilles Tendon. , 2021, , .		0
135	Wavenumber-domain Ultrasonic Imaging of the Bone Cortex Based on Velocity Distribution Estimation. , 2021, , .		0
136	Deep Learning Based Real-time Segmentation in Ultrasonic Imaging Following the Doctor's Voice Guide. , 2021, , .		0
137	Signal Processing Techniques Applied to Axial Transmission Ultrasound. Advances in Experimental Medicine and Biology, 2022, 1364, 95-117.	1.6	0